Electronic Supplementary Material (ESI) for Organic & Biomolecular Chemistry.
This journal is © The Royal Society of Chemistry 2022

Supporting Information

1,2,3-Triazine formation mechanism of a fairy chemical 2-azahypoxanthine in the fairy ring-forming fungus *Lepista sordida*

Akinobu Ito,‡[ab] Jae-Hoon Choi,‡[acd] Waki Yokoyama-Maruyama,[c] Mihaya Kotajima,[a] Jing Wu,[d] Tomohiro Suzuki,[e] Yurika Terashima,[c] Hyogo Suzuki,[c] Hirofumi Hirai,[acd] David C. Nelson,[f] Yuta Tsunematsu,[g] Kenji Watanabe,[g] Tomohiro Asakawa,[h] Hitoshi Ouchi,[g] Makoto Inai,[g] Hideo Dohra[cd] and Hirokazu Kawagishi*[acd]

Correspondence to: kawagishi.hirokazu@shizuoka.ac.jp

[a]*Graduate School of Science and Technology,* [c]*Graduate School of Integrated Science and Technology, and* [d]*Research Institute of Green Science and Technology, Shizuoka University, 836 Ohya, Suruga-ku, Shizuoka 422-8529, Japan*
[b]*Research Fellow of Japan Society for the Promotion of Science, 5-3-1 Kojimachi, Chiyoda-ku, Tokyo 102-0083, Japan*
[e]*Center for Bioscience Research and Education, Utsunomiya University, 350 Minemachi, Tochigi 321-8505, Japan*
[f]*Department of Botany and Plant Sciences, University of California, Riverside, California 92521, USA*
[g]*Department of Pharmaceutical Sciences, University of Shizuoka, 52-1 Yada, Suruga-ku, Shizuoka 422-8526, Japan*
[h]*Marine Science and Technology, Tokai University, 4-1-1 Kitakaname, Hiratsuka City, Kanagawa 259-1292, Japan*

Contents:

Experimental
Tables. S1 and S2
Figs. S1 to S13

General Experimental Procedures. LC-MS/MS analyses were performed with a UPLC system (Shimadzu) coupled with a tandem LTQ Orbitrap mass spectrometer (Thermo Fisher Scientific), and a UPLC system (Nihon Waters) coupled with a tandem Xevo TQ-S micro mass spectrometer (Nihon Waters). HPLC separation was performed with a Jasco Gulliver system using RP-HPLC columns (Develosil C30-UG-5, Nomura Chemical; Cosmosil 5-PYE waters, Nacalai Tesque). An ODS gel (Cosmosil 140 C18-OPN, Nacalai Tesque) was used for flash column chromatography. AHXR was synthesized according to the method previously described.[1] All solvents used throughout the experiments were obtained from Kanto Chemical. The mycelia of *L. sordida* (NBRC 112841) were preincubated on a potato dextrose agar (PDA) medium at 25 °C for a month, and then the mycelial plate was stored at 4 °C until further use.

Feeding Studies Using 20 Kinds of Amino Acids and a NOS Inhibitor. Three fungal pieces (6.0 mm diameter) were inoculated into 100 mL Erlenmeyer flasks containing 30 mL of medium A (0.05% yeast extract and 0.5% D-glucose). One milliliter of 30 mM amino acids and 15 mM L-NAME (Dojindo) filtered through a membrane filter was added into the cultures, and the mycelia were incubated (25 °C, 120 rpm). The amounts of AHX and ICA in the culture broth were analyzed by RP-HPLC. 180 μL of the culture broth was sampled, 20 μL of 1 mM allopurinol (Wako Pure Chemical) was added as an internal standard, and then the sample was analyzed (column, Develosil C30-UG-5, ϕ4.6 × 250 mm; solvent, H_2O; column oven, 28 °C; flow rate, 0.75 mL/min; UV detection, 210, 254, and 275 nm).

Isolation and Detection of ^{15}N-labeled AHX. 30 mycelial disks (6.0 mm diameter) were placed into 500 mL Erlenmeyer flasks including 250 mL of medium A. After preincubation of the mycelia for 3 days, one milliliter of 62.5 mM [guanidino-$^{15}N_2$] L-Arg (Cambridge Isotope Laboratories) or unlabeled L-Arg was added (final 250 μM), and the cultures were further incubated for a month (25 °C, 120 rpm). The culture broth (1 L) was filtered and evaporated under reduced pressure. The concentrate (900.1 mg) was fractionated by ODS gel flash column chromatography: 5% (fractions 1–5), 10% (fractions 6–10), 25% (fractions 11–15), 50% (fractions 16–20) MeOH, and MeOH (fractions 21–25) to obtain 25 fractions (fractions 1–25). Fractions 6–8 were combined and the fraction (42.3 mg) was separated by RP-HPLC (column, Develosil C30-UG-5, ϕ20 × 250 mm; solvent, H_2O; flow rate, 4.0 mL/min; column oven, 28 °C; UV detection, 210, 254, and 275 nm). Subsequently, AHX-containing fractions were combined and the fraction (29.1 mg) was further separated by RP-HPLC (column, Cosmosil 5-PYE waters, ϕ10 × 250 mm; solvent, 2% MeOH; flow rate, 1.5 mL/min; column oven, 28 °C; UV detection, 210, 254, and 275 nm) to afford AHX (6.1 mg). Purified AHX was dissolved with 80% MeCN in 0.05% formic acid (FA) and subjected to LC-MS/MS (Thermo Fisher Scientific). A PC-HILIC column (ϕ2.0 × 100 mm, Osaka Soda) was used (solvent, 95% MeCN in 0.05% FA; column oven, 40 °C; flow rate, 0.2 mL/min). MS analysis was performed in the negative mode with the following source parameters: sheath gas flow, 50 arb; auxiliary gas flow, 10 arb; tube lens, –42 V; capillary voltage, –1.0 V; ion spray voltage, 3.0 kV; capillary temperature, 350 °C. MS spectra were detected by Orbitrap fourier transform mass spectrometer (Orbitrap FT-MS), and MS/MS spectra were detected by linear ion trap quadrupole mass spectrometer (LTQ-MS). AHX was identified by exact mass and characteristic transition (precursor ion to daughter ion).

RNA Sequencing of *L. sordida*. *L. sordida* was cultured as described in the previous report.[2] Total RNA was extracted from the mycelia using TRIzol (Thermo Fisher Scientific) and

incubated with deoxyribonuclease I (Thermo Fisher Scientific) for 15 min at room temperature, and then EDTA was added (final 2.5 mM) into the mixture. Total RNA was further purified using RNeasy Mini Kit (Qiagen). Libraries for strand-specific RNA sequencing were constructed using SureSelect Strand-specific RNA Library Prep Kit (Agilent Technologies), according to the manufacturer's instruction. The libraries were sequenced using a MiSeq platform (Illumina) to generate 2 × 76-bp paired-end sequence reads. The raw sequence reads have been deposited in DDBJ Sequence Read Archive (DRA) under the accession number (DRR252166). The raw read sequences were cleaned up using Trimmomatic (ver. 0.36) by trimming adapter sequence, the 76th base at the end of the reads, and the low-quality (quality, < 15) and shortened (length, < 50 bp) reads were removed.[3] The resulting high-quality reads totaling 1,283 Mb were aligned to the draft genome sequence of *L. sordida* (Genbank accession number, BIMQ00000000.1) using HISAT2 (ver. 2.2.0) with options of a minimum intron length of 20 bp and a maximum intron length of 5,000 bp.[4] The *LsNOS* genes were predicted using BRAKER1 (ver. 1.9) with the aligned RNA-seq data with a --fungus option.[5] In the BRAKER1 pipeline, GeneMark-ET created an *ab initio* gene set, and then AUGUSTUS predicted an improved gene set using spliced alignment information from the RNA-seq data.[6, 7] The predicted *LsNOS* genes were manually curated based on the visualization of the aligned RNA-seq data using Integrative Genomics Viewer (IGV).[8]

***LsNOS* Gene Expression Analysis.** The expression level of *LsNOS* genes was estimated using the RNA-seq data. Read counts mapped to the *LsNOS* genes were calculated from the aligned RNA-seq data using featureCounts (ver. 2.0.0), and TPM values were calculated in order to normalize transcript lengths and total read counts.[9]

Structural Analysis of NOS Proteins. Amino acid sequences of LsNOS proteins were analyzed by InterProScan (http://www.ebi.ac.uk/interpro/) to identify their protein families and functional domains.[10] To estimate the L-Arg/NOHA binding abilities of LsNOSs, amino acid sequences of the NOS_oxygenase domain (cd00575) of LsNOSs, mouse iNOS (NP_035057), and *B. subtilis* NOS (O34453.2) were aligned using MAFFT (ver. 7.450) and visualized using Geneious Prime 2020.[11, 12]

Phylogenetic Analysis of LsNOS Proteins. The phylogenetic relationship of LsNOS proteins was analyzed based on the NOS_oxygenase domain (cd00575) in Conserved Domain Database. 57 NOS_oxygenase domains from *L. sordida* and other species listed in Supplementary Table 1 were aligned using MAFFT (ver. 7.450).[12] A maximum likelihood phylogenetic tree was reconstructed using IQ-TREE (ver. 1.6.12) with the best-fit model (LG+I+G4) with 1,000 replicates of the ultrafast bootstrap using UFBoot2 implemented in IQ-TREE.[13, 14]

Heterologous Expression of rLsNOS Proteins. Two *L. sordida* disks (8.5 mm diameter) were inoculated into 10 mL of medium B (0.3% yeast extract, 1% D-glucose, 0.05% Na_2HPO_4, 0.05% KH_2PO_4, and pH 5.5) supplemented with unlabeled L-Arg (final 1 mM) and cultured for 1 week (25 °C, 120 rpm). Total RNA was prepared as described above, and then cDNA was reverse-transcribed from 500 ng of total RNA using Prime Script RT Reagent Kit Perfect Real Time (TaKaRa Bio). Full-length cDNA fragments of *LsNOS2* and *LsNOS8* genes were amplified by RT-PCR using PrimeSTAR Max DNA polymerase (TaKaRa Bio). All primers used in this experiment were listed in Supplementary Table 2. The reaction mixture (10 μL) contained 50 ng of total cDNA, 5 μL of the polymerase, and 0.3 μM each primer. Cycling conditions were set as

the follows: preincubation, one cycle of 94 °C for 2 min; amplification, 35 cycles of 98 °C for 10 s, 60 °C for 15 s, and 72 °C for 30 s (for *LsNOS2* gene) or 15 s (for *LsNOS8* gene). The amplified PCR products were cloned into pET21c(+) expression vector (Sigma-Aldrich Japan) between *Nde*I and *Xho*I sites using Gibson Assembly Master Mix (New England BioLabs Japan) to afford expression plasmids pCK1009 (pET21c(+)-*LsNOS2*) and pKW20700 (pET21c(+)-*LsNOS8*), which were transformed into *E. coli* DH5α (Nippon Gene). The plasmids were extracted with HiYield Plasmid Mini Kit (RBC Bioscience). Authenticity of the extracted plasmids was confirmed by PCR and sequencing, followed by transformation into *E. coli* BL21 (DE3) (Nippon Gene) for the pCK1009 expression or into *E. coli* SHuffle T7 express (New England BioLabs Japan) for the pKW20700 expression. Cells harboring the corresponding plasmid were grown overnight (37 °C, 200 rpm) in LB medium containing 100 μg/mL ampicillin. The culture (10 mL) was added into TB medium containing the antibiotic, and the culture (1 L) was incubated (37 °C, 150 rpm) until OD_{600} reached 0.3. 5-Aminolevulinic acid (Wako Pure Chemical) (final 1 mM) and $FeSO_4 \cdot 7H_2O$ (final 100 μM) were added, and the culture was further incubated until OD_{600} reached 0.6 and then was cooled to 16 °C. Recombinant protein expression was induced by 0.1 mM isopropyl β-D-1-thiogalactopyranoside (IPTG) and the cells were cultured (16 °C, 130 rpm) for at least 40 h. The cells were harvested by centrifugation and stored at –80 °C until protein extraction.

Purification of rLsNOS Proteins. *E. coli* cells were suspended in extraction buffer (20 mM Tris-HCl, pH 7.4, 500 mM NaCl, 10% glycerol, and 30 mM imidazole). After lysis by sonication for 15 min on ice, the cell debris was removed by centrifugation. The supernatant was filtered using a membrane filter and subjected to Ni affinity column chromatography using HisTrap HP (GE Healthcare Japan) on NGC Chromatography System (Bio Rad). After washing the column with wash buffer (20 mM Tris-HCl, pH 7.4, 500 mM NaCl, 10% glycerol, and 50 mM imidazole), the His-tagged protein was eluted with elution buffer (20 mM Tris-HCl, pH 7.4, 500 mM NaCl, 10% glycerol, and 1 M imidazole) with a linear gradient program (from 50 mM to 500 mM imidazole). The recombinant protein eluted fractions were confirmed by 10% SDS-PAGE and were desalted against dialysis buffer (20 mM Tris-HCl, pH 7.4, 500 mM NaCl, and 10% glycerol) at 4 °C. After dialysis, the protein solution was concentrated and replaced with enzyme buffer (100 mM Tris-HCl, pH 7.4, 500 mM NaCl, and 20% glycerol) using Amicon Ultra-0.5 mL 10K (Merck). The purified protein concentration was quantified using Pierce 660 nm Protein Assay Reagent (Thermo Fisher Scientific) with BSA as a standard, and the enzyme was stored at –80 °C until further used.

Refolding of rLsNOS2 Protein. *E. coli* cells were extracted using the same extraction method described above, and the cell debris was recovered by centrifugation. Based on the refolding methods of plant and fungal recombinant peroxidases, a refolding mixture (20 mL) containing 5 mg of protein, 3 M urea, 50 mM Tris-HCl (pH 9.5), 10% glycerol, 0.7 mM glutathione disulfide (Tokyo Chemical Industry), 0.2 mM glutathione (Tokyo Chemical Industry), and 10 μM hemin (Tokyo Chemical Industry) was prepared.[15-17] The mixture was incubated at 4 °C for 24 h and desalted against dialysis buffer (20 mM Tris-HCl, pH 7.4, 500 mM NaCl, and 10% glycerol). After dialysis, the filtered protein solution was purified as described above.

Enzyme Assay for rLsNOSs. An enzyme reaction mixture (30 μL) contained 5 μM rLsNOSs, 1 mM N^G-hydroxy-L-Arg (Sigma-Aldrich Japan) or L-Arg, 40 mM H_2O_2 (Wako Pure Chemical),

and 50 mM HEPES-NaOH (pH 7.0).[18] The reaction was initiated by adding H_2O_2 and terminated with 20 μL of catalase (200 Units) (Wako Pure Chemical). The reaction mixture was incubated for 15 min at room temperature. Production of nitrite was determined using Nitrate/Nitrite Colorimetric Assay Kit (Cayman Chemical), which is based on reaction of nitrite with Griess reagents containing sulfanilamide and *N*-(1-naphthyl)ethylenediamine.[19] For the synthesis of AHXR and AHX, an enzyme reaction mixture (100 μL) including 10 μM rLsNOS2, 1 mM N^G-hydroxy-L-Arg, 0.2 mM AICAR (Sigma-Aldrich Japan) or AICA (Wako Pure Chemical), 40 mM H_2O_2, and 50 mM HEPES-NaOH (pH 7.0) or CH_3COONa-CH_3COOH (pH 4.0) was prepared. A mixture containing cPTIO (final 10 mM) (Dojindo) was used as a negative control. After incubation at room temperature for 3 h, the reaction was quenched by addition of catalase. Subsequently, the mixture was boiled for 5 min and centrifuged to precipitate protein, and then the supernatant was subjected to LC-MS/MS (Nihon Waters). A CAPCELL PAK ADME S3 column (ϕ2.1 × 250 mm, Osaka Soda) was used in this analysis (solvent, A: 10 mM ammonium formate, B: MeOH, 2% solvent B; column oven, 40 °C; flow rate, 0.2 mL/min). For AHXR detection, MS analysis was performed in the positive mode: capillary voltage, 2.0 kV; cone voltage, 16 V; collision energy, 16 V. For AHX detection, MS analysis was performed in the positive mode: capillary voltage, 2.0 kV; cone voltage, 26 V; collision energy, 16 V. The following source parameters were common to both of the compounds: desolvation temperature, 500 °C; desolvation gas flow, 1000 L/h; cone gas flow, 50 L/h.

Non-enzymatic Reaction from AICA to AHX. For a non-enzymatic assembly using NOC5, a reaction mixture (100 μL) including 1 mM AICA and 0.5 mM NOC5 (Dojindo) in water was prepared, and the mixture was incubated at room temperature for 1 h. A mixture in which NOC5 and cPTIO (final 5 mM) were preincubated for 10 min before adding AICA was used as a negative control. After incubation, AHX was detected by LC-MS/MS (Thermo Fisher Scientific) in the same method above. For a non-enzymatic reaction (100 μL) using sodium nitrite, AICA (final 1 mM) and sodium nitrite (final 1 mM) were incubated in 50 mM CH_3COONa-CH_3COOH (pH 5.0), PIPES-NaOH (pH 6.0), or HEPES-NaOH (pH 7.0) at 30 °C for 3 h. After incubation, AHX was detected by UPLC (Nihon Waters) (column, CAPCELL PAK ADME S3; solvent, A: 10 mM ammonium formate, B: MeOH, 2% solvent B; column oven, 40 °C; flow rate, 0.2 mL/min; UV detection, 254 nm).

Labeling Studies Using ^{15}N-labeled Sodium Nitrite and Sodium Nitrate. Two fungal pieces (8.5 mm diameter) were inoculated into 50 mL Erlenmeyer flasks containing 10 mL of medium A. One milliliter of ^{15}N-labeled sodium nitrite (Cambridge Isotope Laboratories), unlabeled sodium nitrite, ^{15}N-labeled sodium nitrate (Shoko Science), unlabeled sodium nitrate, and unlabeled L-Arg filtered through a membrane filter was added into the cultures (final 1 mM), and the mycelia were incubated (25 °C, 120 rpm). The production of AHX and ICA in the culture broth was analyzed by UPLC as described above. ^{15}N-labeled AHX was detected by LC-MS/MS (Thermo Fisher Scientific).

Table S1 57 kinds of NOSs used in this study.

Organism	Accession	Description	Length (AA)
Streptomyces pathocidini	QIQ51167.1	PtnF	390
Bacillus subtilis subsp. subtilis str. 168	O34453.2	nitric oxide synthase oxygenase	363
Physarum polycephalum	AAK43730.1	nitric oxide synthase form A	1055
Physarum polycephalum	AAK43729.2	nitric oxide synthase form B	1046
Coniosporium apollinis CBS 100218	XP_007784567.1	hypothetical protein W97_08510	1088
Botryosphaeria dothidea	KAF4306495.1	hypothetical protein GTA08_BOTSDO05762	1060
Microthyrium microscopicum	KAF2672562.1	hypothetical protein BT63DRAFT_396259	1071
Viridothelium virens	KAF2236995.1	hypothetical protein EV356DRAFT_512271	1147
Venturia nashicola	TID14058.1	nitric oxide synthase-like protein	1011
Cercospora zeina	PKR97087.1	nitric oxide synthase	1049
Dothistroma septosporum NZE10	EME47190.1	hypothetical protein DOTSEDRAFT_77571	1111
Zymoseptoria tritici ST99CH_1A5	SMY24840.1	unnamed protein product	1126
Aulographum hederae CBS 113979	KAF1990629.1	hypothetical protein K402DRAFT_410120	1046
Lepidopterella palustris CBS 459.81	OCK79887.1	hypothetical protein K432DRAFT_454237, partial	1035
Tothia fuscella	KAF2433829.1	hypothetical protein EJ08DRAFT_583262	1089
Verruconis gallopava	XP_016209150.1	hypothetical protein PV09_09048	1165
Aspergillus oryzae RIB40	XP_001825673.2	nitric oxide synthase	1024
Aspergillus flavus NRRL3357	XP_002381643.1	nitric oxide synthase, putative	1024
Letharia columbiana	KAF6239642.1	hypothetical protein HO173_002188	1121
Oidiodendron maius Zn	KIM93262.1	hypothetical protein OIDMADRAFT_138126	1024
Colletotrichum graminicola M1.001	EFQ35699.1	nitric oxide synthase	1058
Ophiocordyceps sinensis CO18	EQL02386.1	nitric oxide synthase	1047
Coniochaeta ligniaria NRRL 30616	OIW33174.1	hypothetical protein CONLIGDRAFT_666516	1053
Pseudomassariella vexata	ORY71769.1	nitric oxide synthase	1053
Dendrothele bispora CBS 962.96	THU86598.1	hypothetical protein K435DRAFT_868134	1025
Pterula gracilis	TFK98355.1	nitric oxide synthase	973
Lepista sordida LsNOS1	GHP15256.1	nitric oxide synthase, putative	1061
Lepista sordida LsNOS2	GHP15257.1	nitric oxide synthase, putative	961
Lepista sordida LsNOS3	GHP15258.1	nitric oxide synthase, putative	804
Lepista sordida LsNOS4	GHP15259.1	nitric oxide synthase, putative	1113
Lepista sordida LsNOS5	GHP15260.1	nitric oxide synthase, putative	811
Lepista sordida LsNOS6	GHP15261.1	nitric oxide synthase, putative	667
Lepista sordida LsNOS7	GHP15262.1	nitric oxide synthase, putative	1109
Lepista sordida LsNOS8	GHP15263.1	nitric oxide synthase, putative	471
Rhizoctonia solani AG-3 Rhs1AP	EUC55953.1	nitric oxide synthase, inducible protein, partial	1045
Branchiostoma floridae	XP_035673410.1	nitric oxide synthase, brain-like	1329
Branchiostoma floridae	XP_035691848.1	nitric oxide synthase, brain-like isoform X1	1476
Danio rerio	NP_001098407.1	nitric oxide synthase 2a, inducible	1079
Danio rerio	NP_001106973.1	nitric oxide synthase 2b, inducible	1077
Danio rerio	NP_571735.1	nitric oxide synthase, brain	1431
Xenopus tropicalis	XP_004910558.1	nitric oxide synthase, brain isoform X1	1420
Xenopus tropicalis	NP_001243158.1	nitric oxide synthase, endothelial	1177
Xenopus tropicalis	XP_002935342.2	nitric oxide synthase, inducible	1160
Gallus gallus	XP_004934537.3	nitric oxide synthase, brain isoform X1	1435
Gallus gallus	XP_025003142.1	nitric oxide synthase, endothelial	1171
Gallus gallus	NP_990292.1	nitric oxide synthase, inducible	1136
Mus musculus	NP_032738.1	nitric oxide synthase, brain	1429
Mus musculus	NP_032739.3	nitric oxide synthase, endothelial	1202
Mus musculus	NP_035057.1	nitric oxide synthase, inducible isoform a	1144
Homo sapiens	NP_000611.1	nitric oxide synthase, brain isoform 1	1434
Homo sapiens	NP_000594.2	nitric oxide synthase, endothelial isoform 1	1203
Homo sapiens	NP_000616.3	nitric oxide synthase, inducible	1153
Ciona intestinalis	XP_009861972.2	nitric oxide synthase, brain-like	1364
Nematostella vectensis	XP_032236179.1	nitric oxide synthase, brain isoform X1	1394
Daphnia magna	XP_032789253.1	nitric oxide synthase, salivary gland-like isoform X1	1127
Drosophila melanogaster	NP_523541.2	nitric oxide synthase, isoform A	1349
Ostreococcus lucimarinus CCE9901	XP_001421937.1	predicted protein	1059

Table S2 Primers used in this study.

Primer name	Sequence (5' to 3')	Description
pCK1009-F	AGAAGGAGATATACAATGGGTAGTGTCAT TTGCCCCTTTGC	Expression of LsNOS2 gene
pCK1009-R	TCAGTGGTGGTGGTGGTGGTGGTGGTGGT GCCCGAATACTTCTTCGACATATCTGACC CCCATAGTTTTC	Expression of LsNOS2 gene
pKW20700-F	AGAAGGAGATATACAATGGGTACCGTTAT CTGCCCTCATGC	Expression of LsNOS8 gene
pKW20700-R	TCAGTGGTGGTGGTGGTGGTGGTGGTGG CGCCATATTCGCAGCGCTAAAGAATTTTGCG	Expression of LsNOS8 gene

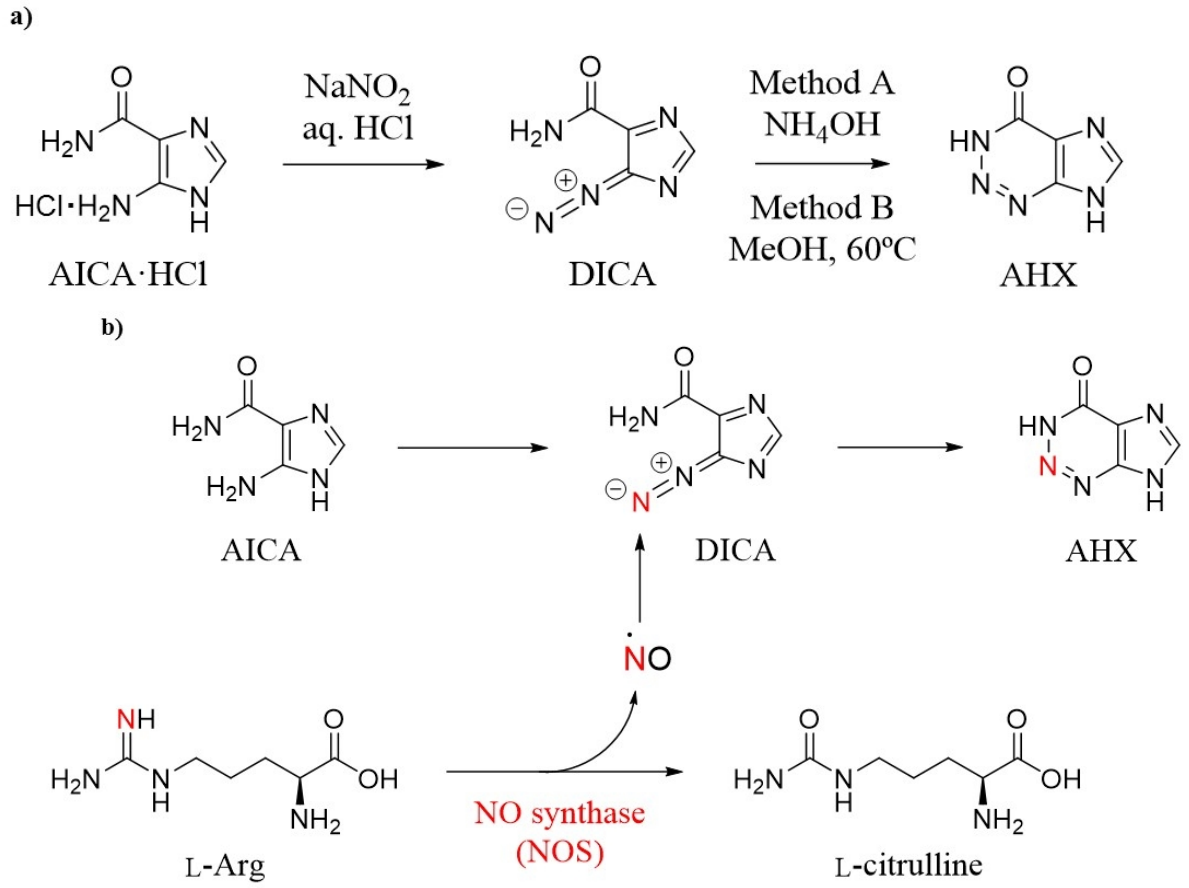

Fig. S1 a) Chemical synthesis of AHX, and **b)** putative biosynthetic pathway to AHX in *L. sordida*. Methods A and B are described in the references 27 and 29, respectively.

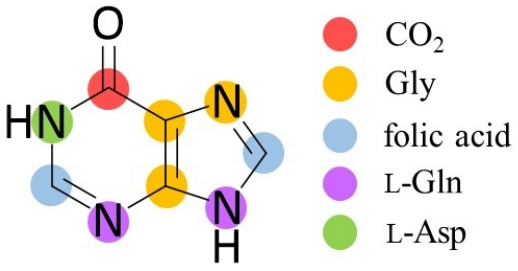

Fig. S2 Biosynthetic origin of the purine skeletons.

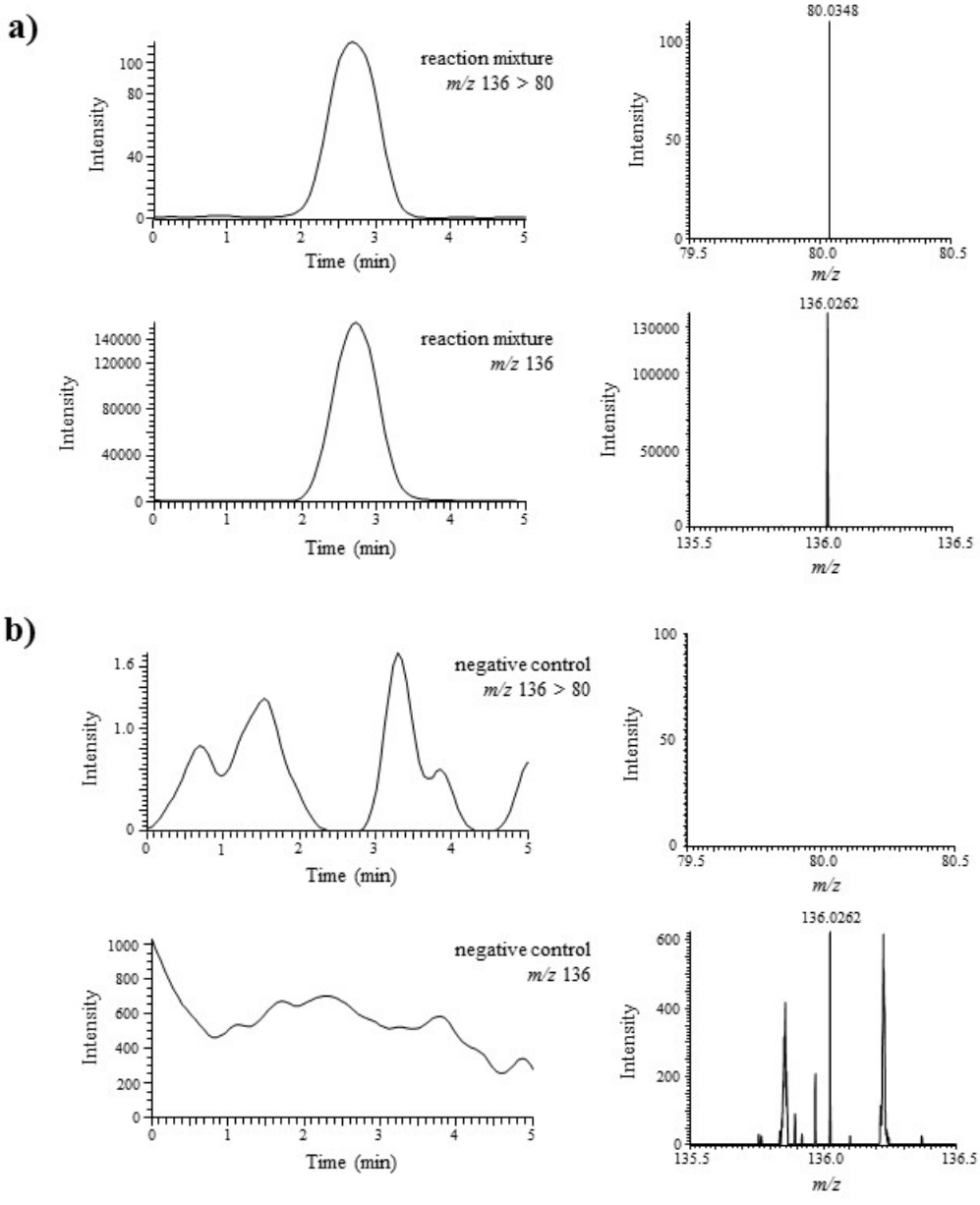

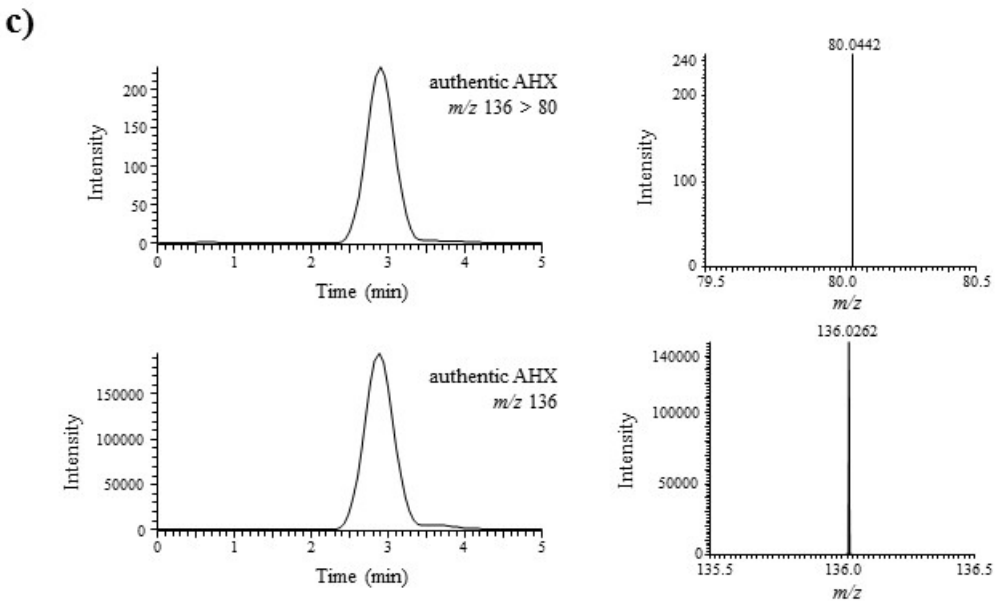

Fig. S3 Non-enzymatic conversion from AICA to AHX in presence of an NO donor (NOC5). AHX was detected in the negative mode by LC-MS/MS. LC-MS (bottom) and LC-MS/MS (top) chromatograms, and MS spectra of AHX are shown. **a)** AICA and the donor reaction mixture, **b)** negative control, and **c)** authentic standard. A mixture in which the donor and cPTIO (an NO scavenger) were preincubated before adding of AICA was used as the negative control. MS spectra were detected by Orbitrap fourier transform mass spectrometer (Orbitrap FT-MS) and MS/MS spectra were detected by linear ion trap quadrupole mass spectrometer (LTQ-MS). AHX was identified by exact mass and characteristic transition (precursor ion to daughter ion).

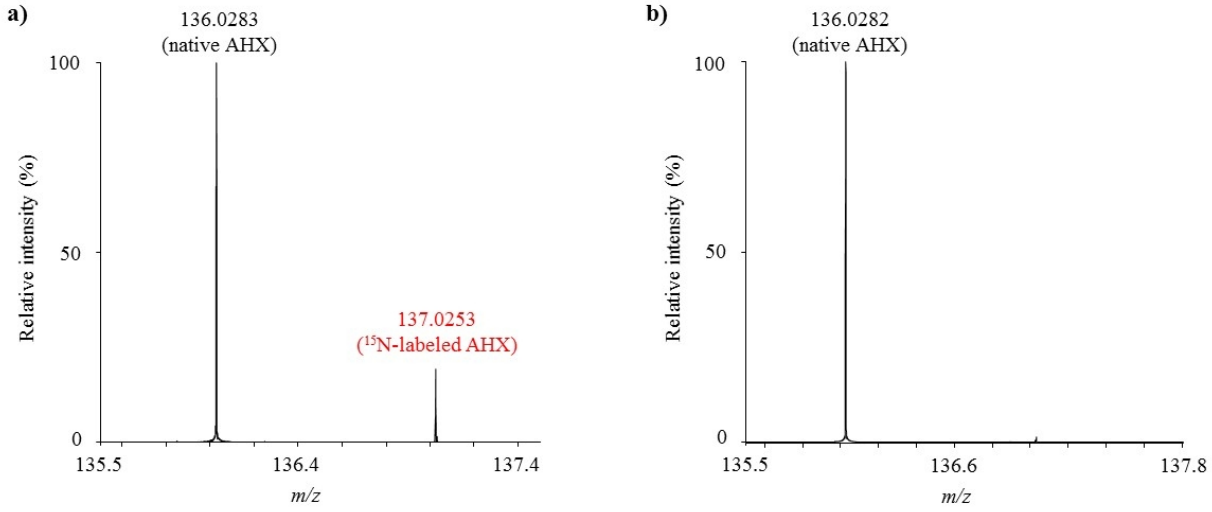

Fig. S4 MS spectra of AHX derived from [guanidino-$^{15}N_2$] L-Arg. **a)** AHX fraction from the culture broth treated with labeled L-Arg. **b)** AHX fraction from the culture broth after incubation with unlabeled L-Arg. The culture broth was fractionated by the high-sensitivity detection method for FCs described in the reference 10. Red highlight indicates AHX come from the labeled amino acid. MS spectra were detected by Orbitrap FT-MS. AHX was detected in the negative mode.

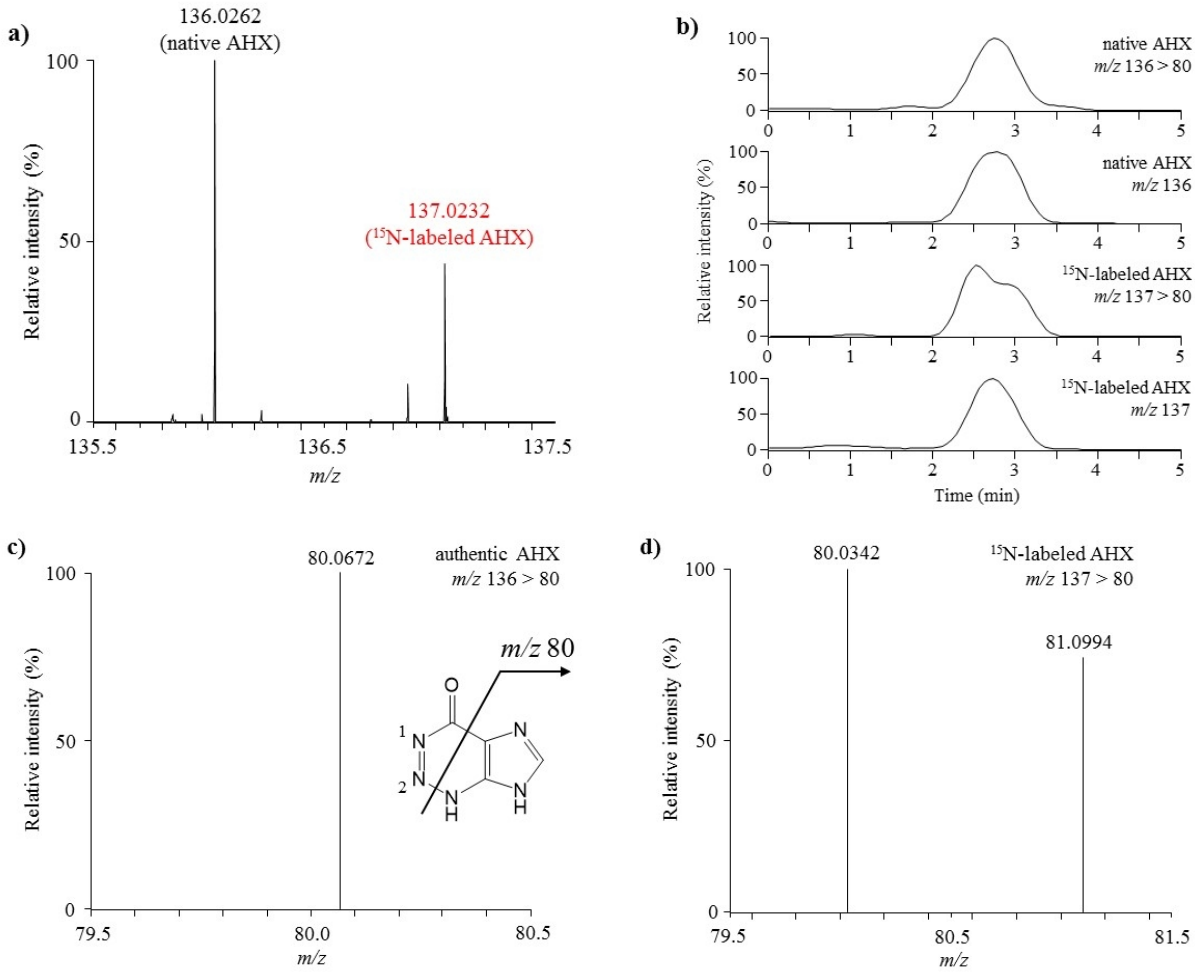

Fig. S5 Identification of ^{15}N-labeled AHX derived from [guanidino-$^{15}N_2$] L-Arg by LC-MS/MS. **a)** MS spectrum of AHX purified from the culture broth treated with labeled L-Arg. Red highlight indicates the signal of AHX come from the labeled amino acid. **b)** LC-MS/MS chromatograms of purified AHX. First and second rows indicate LC-MS/MS and LC-MS chromatograms of unlabeled AHX, and third and fourth rows indicate those of ^{15}N-labeled AHX, respectively. **c)** MS/MS spectrum of authentic AHX. **d)** MS/MS spectrum of ^{15}N-labeled AHX. MS spectrum was detected by Orbitrap FT-MS, and MS/MS spectra were detected by LTQ-MS. AHX was detected in the negative mode and identified by exact mass and characteristic transition.

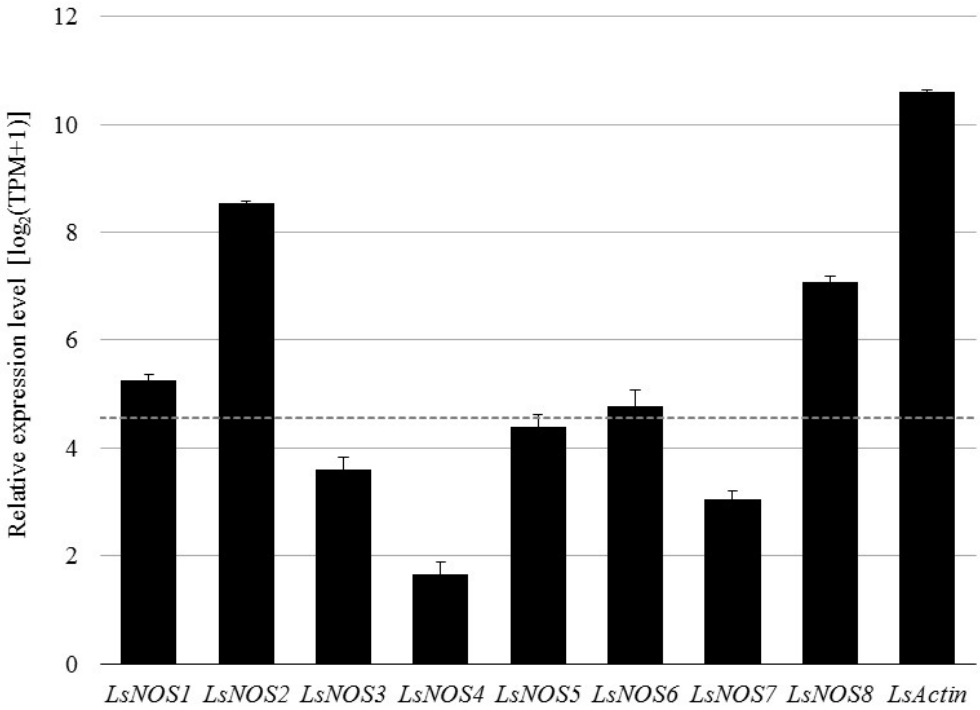

Fig. S6 Relative expression level of LsNOS genes. Transcripts per million (TPM) values were calculated from read counts mapped to the LsNOS and LsActin (GHP15264.1) genes based on the aligned RNA-seq data. Results are means of $\log_2$(TPM+1) ± standard deviations (n = 3). Dash line shows the median expression level of all the protein-coding genes.

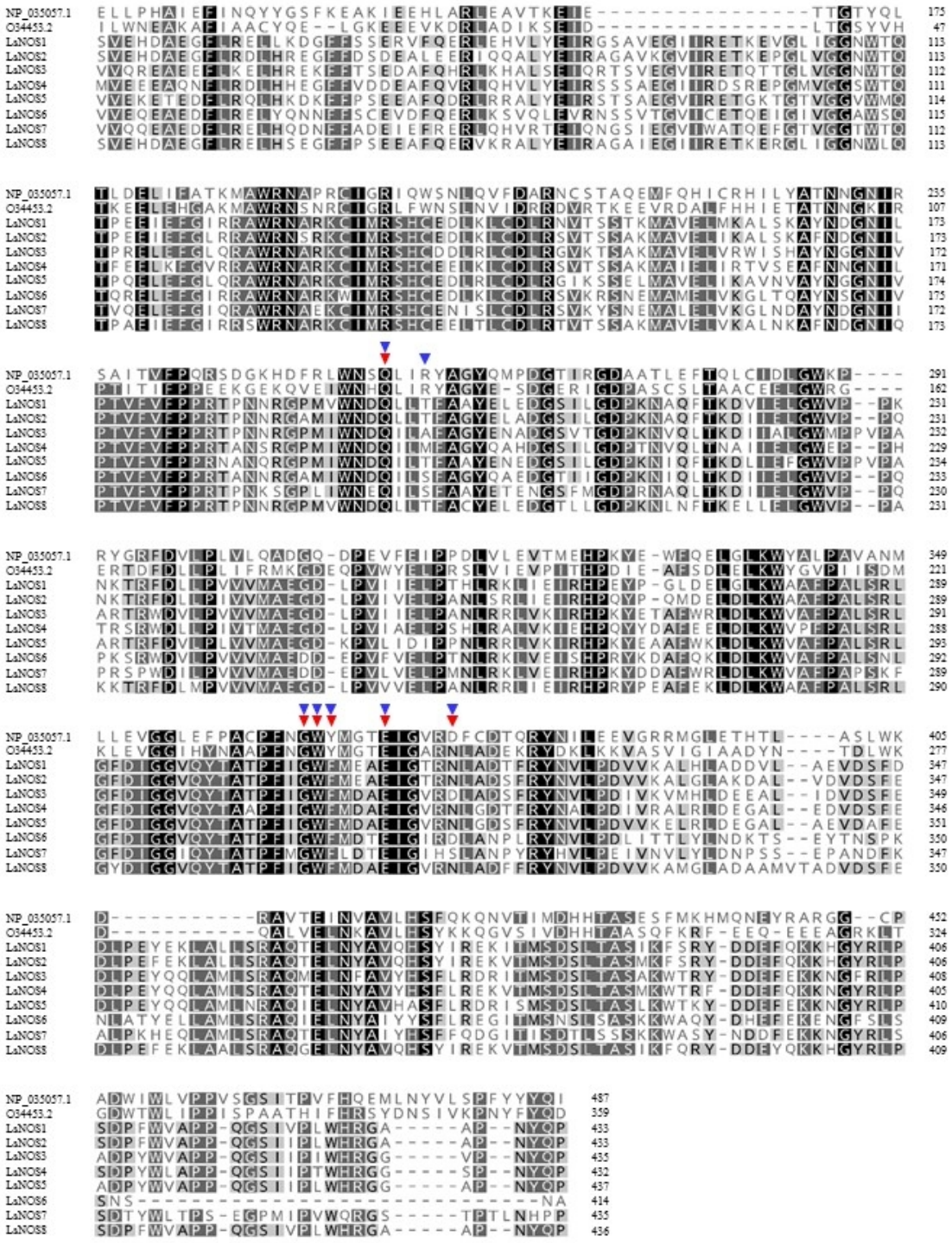

Fig. S7 Amino acid sequence alignment of the NOS_oxygenase domain of NOSs. The NOS_oxygenase domain of mouse iNOS (accession number, NP_035057.1) and *Bacillus subtilis* NOS (accession number, O34453.2) were used as representatives of metazoan and bacterial NOS, respectively. Amino acid sequences of the NOS_oxygenase domain were aligned using MAFFT and visualized using Geneious, and colors of amino acid residues are shown in grayscale depending on the conservation. Amino acid residues involved in the L-Arg/NOHA binding in mouse iNOS and *B. subtilis* NOS are indicated with red and blue triangles, respectively.

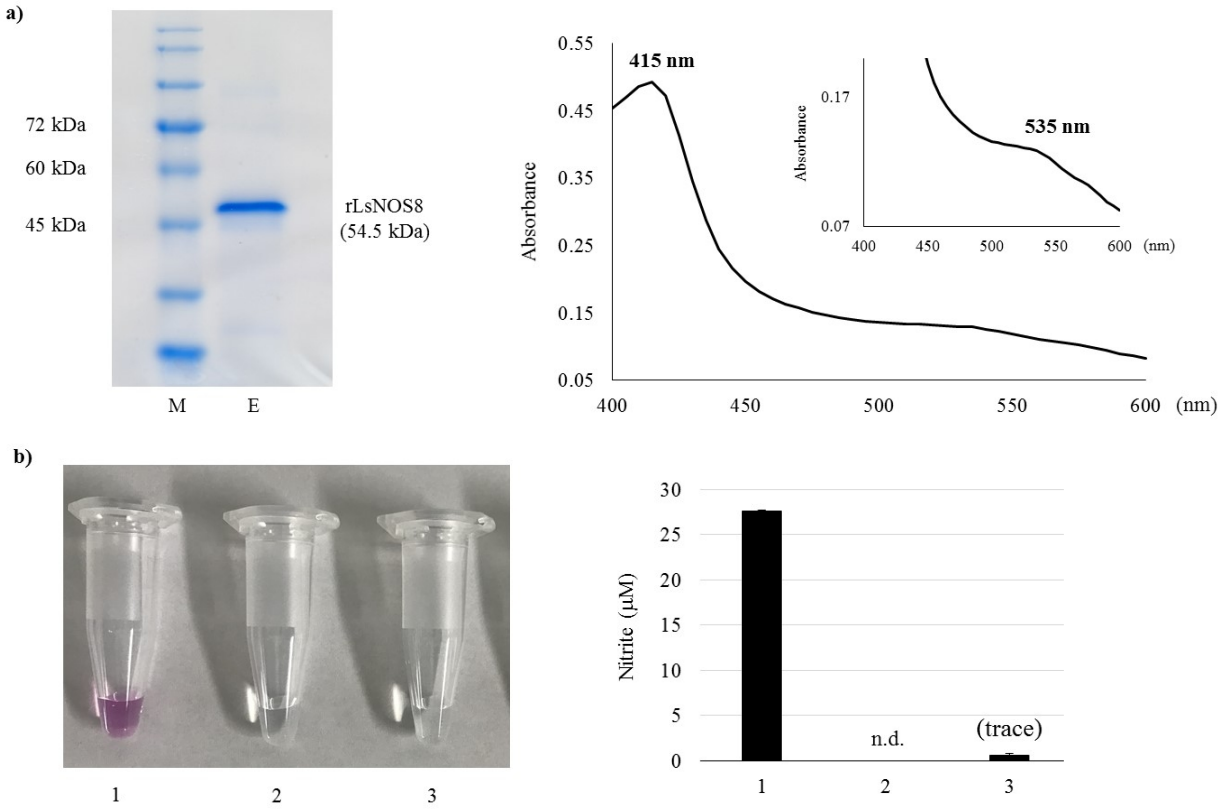

Fig. S8 *In vitro* characterization of rLsNOS8. **a)** SDS-PAGE of purified rLsNOS8 expressed in *E. coli* and UV-vis spectrum of the isolated enzyme. The enzyme was produced as a *C*-terminally His-tagged protein and isolated by Ni affinity column chromatography. Lane M, molecular weight marker; lane E, eluted fraction (a linear gradient from 50 to 500 mM imidazole). The spectrum was recorded by a UV-1900 UV-vis spectrophotometer (Shimadzu). **b)** *In vitro* enzyme assay of rLsNOS8. Nitrite was quantified by Griess reagents as described in Experimental Section. Results are means ± standard errors (n = 3). Lane 1, enzyme reaction; lane 2, reaction mixture without the enzyme; lane 3, reaction mixture without H_2O_2. n.d., not detected.

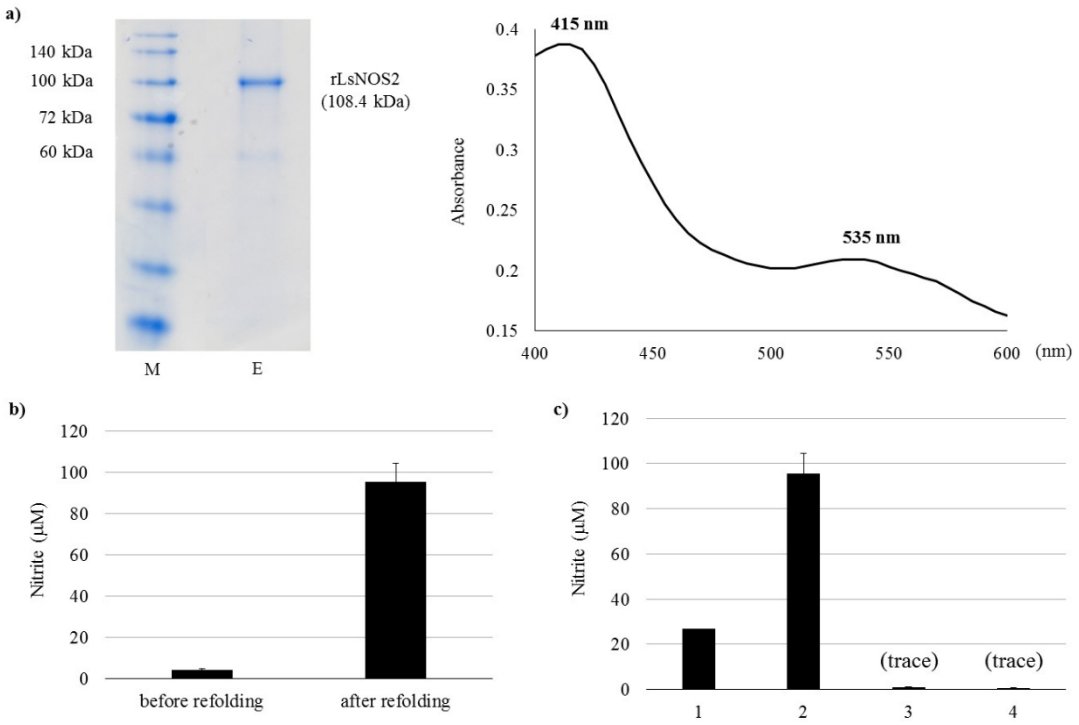

Fig. S9 *In vitro* characterization of rLsNOS2. **a)** SDS-PAGE of purified rLsNOS2 expressed in *E. coli* and UV-vis spectrum of the isolated enzyme. rLsNOS2 was produced as a *C*-terminally His-tagged protein and isolated by Ni affinity column chromatography. Lane M, molecular weight marker; lane E, eluted fraction (a linear gradient from 50 to 500 mM imidazole). The spectrum was recorded by a UV-1900 UV-vis spectrophotometer. **b)** Effect of *in vitro* refolding on the enzyme activity of rLsNOS2. **c)** *In vitro* enzyme assay of rLsNOS2. Nitrite was quantified by Griess reagents as described in Experimental Section. Results are means ± standard errors (n = 3). Lane 1, enzyme reaction of rLsNOS8; lane 2, enzyme reaction of refolded rLsNOS2; lane 3, reaction mixture without the refolded enzyme; lane 4, the refolded enzyme reaction mixture without H_2O_2.

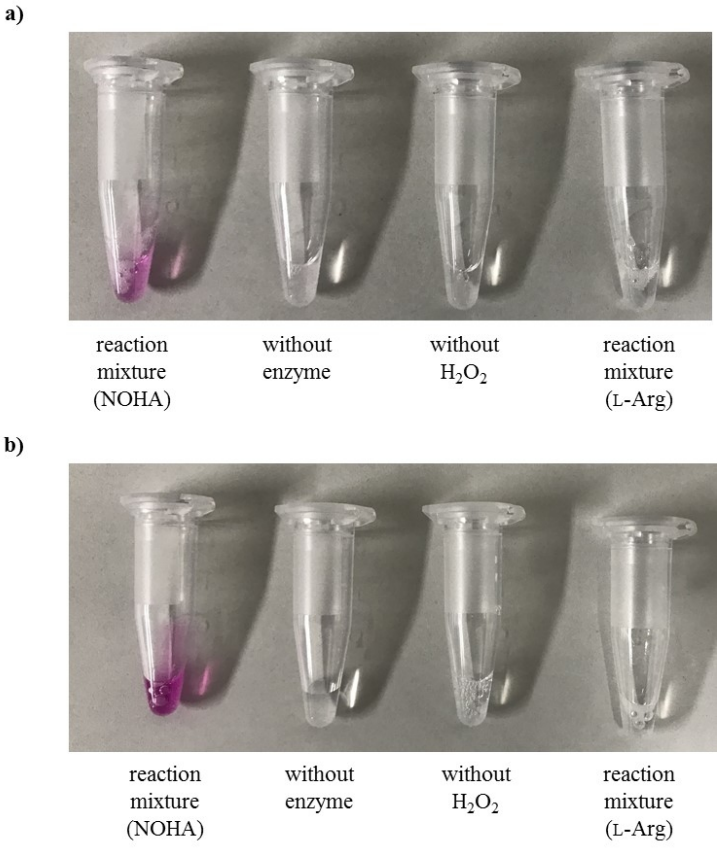

Fig. S10 Detection of nitrite production by rLsNOSs using NOHA or L-Arg as a substrate. **a)** Enzyme assay of rLsNOS8. **b)** Enzyme assay of rLsNOS2. rLsNOS2 which was subjected to *in vitro* refolding described in the references 47–49 was used. Nitrite was quantified by Griess reagents as described in Experimental Section. Reaction mixtures, in which NOHA as a substrate and no enzyme or no H_2O_2 were contained, were used as negative controls.

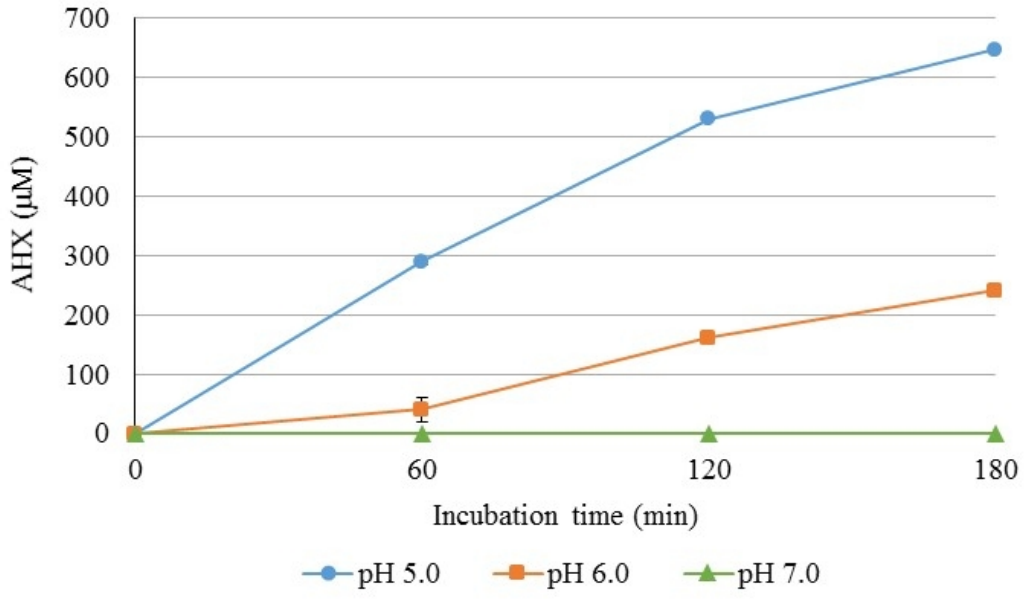

Fig. S11 Effect of pH on the reaction from AICA to AHX. The reaction was carried out with AICA and sodium nitrite at pH 5.0 to 7.0, and the production of AHX was observed below pH 6.0.

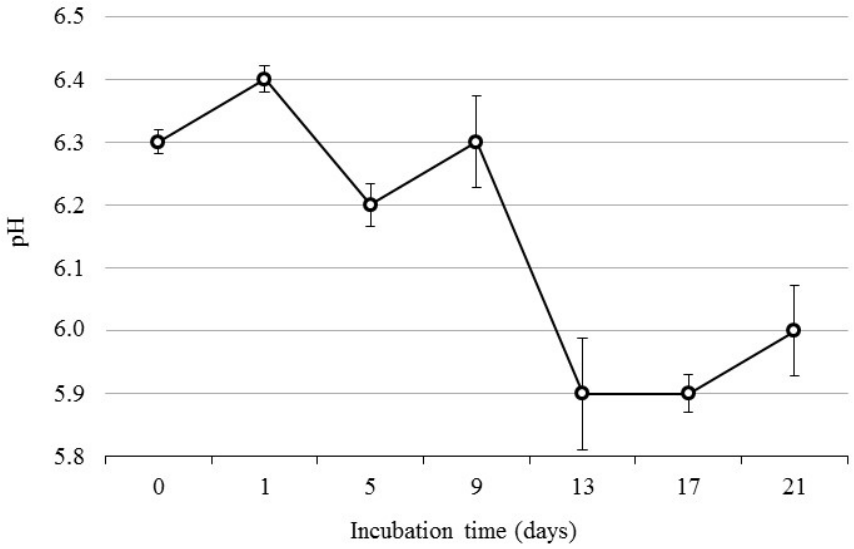

Fig. S12 Variation with time of pH in the *L. sordida* culture. Two mycelial disks (8.5 mm diameter) were inoculated into 50 mL Erlenmeyer flasks containing 10 mL of YG medium (0.3% yeast extract and 1% D-glucose), and the fungus was cultured (25 °C, 120 rpm). Results are means ± standard errors (n = 3).

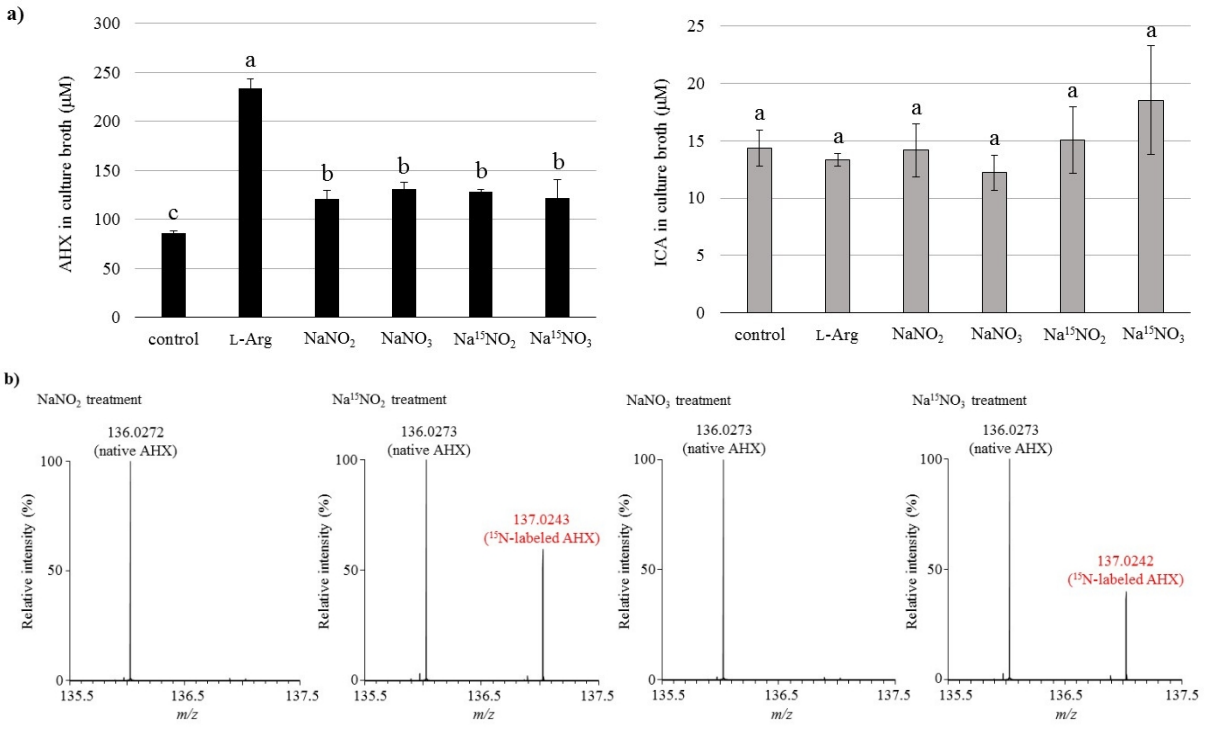

Fig. S13 Effect of ^{15}N-labeled nitrite and nitrate treatment on the production of AHX and ICA by *L. sordida*. **a)** AHX and ICA in the culture broth. The fungus was cultured for 2 weeks, and the culture broth was analyzed by UPLC. Results are means ± standard errors (n = 3). Different alphabets represent statistical significance of difference at 5%. **b)** MS spectra of ^{15}N-labeled AHX derived from ^{15}N-labeled nitrite and ^{15}N-labeled nitrate. Red highlight indicates AHX come from the labeled compounds. MS spectra were detected by Orbitrap FT-MS. AHX was detected in the negative mode and identified by exact mass and characteristic transition.

1. K. Ikeuchi, R. Fujii, S. Sugiyama, T. Asakawa, M. Inai, Y. Hamashima, J.-H. Choi, T. Suzuki, H. Kawagishi and T. Kan, *Org. Biomol. Chem.*, 2014, **12**, 3813-3815.
2. T. Suzuki, N. Yamamoto, J.-H. Choi, T. Takano, Y. Sasaki, Y. Terashima, A. Ito, H. Dohra, H. Hirai, Y. Nakamura, K. Yano and H. Kawagishi, *Sci. Rep.* , 2016, **6**, 39087.
3. A. M. Bolger, M. Lohse and B. Usadel, *Bioinformatics*, 2014, **30**, 2114-2120.
4. D. Kim, J. M. Paggi, C. Park, C. Bennett and S. L. Salzberg, *Nat. Biotechnol.*, 2019, **37**, 907-915.
5. K. J. Hoff, S. Lange, A. Lomsadze, M. Borodovsky and M. Stanke, *Bioinformatics*, 2016, **32**, 767-769.
6. M. Stanke, M. Diekhans, R. Baertsch and D. Haussler, *Bioinformatics*, 2008, **24**, 637-644.
7. A. Lomsadze, P. D. Burns and M. Borodovsky, *Nucleic Acids Res.*, 2014, **42**, e119-e119.
8. J. T. Robinson, H. Thorvaldsdóttir, W. Winckler, M. Guttman, E. S. Lander, G. Getz and J. P. Mesirov, *Nat. Biotechnol.*, 2011, **29**, 24-26.
9. Y. Liao, G. K. Smyth and W. Shi, *Bioinformatics*, 2014, **30**, 923-930.
10. S. El-Gebali, J. Mistry, A. Bateman, S. R. Eddy, A. Luciani, S. C. Potter, M. Qureshi, L. J. Richardson, G. A. Salazar, A. Smart, L. Erik, L. Hirsh, L. Paladin, D. Piovesan, C. Silvio and R. D. Finn, *Nucleic Acids Res.*, 2019, **47**, D427-D432.
11. M. Kearse, R. Moir, A. Wilson, S. Stones-Havas, M. Cheung, S. Sturrock, S. Buxton, A. Cooper, S. Markowitz, C. Duran, T. Thierer, B. Ashton, P. Meintjes and A. Drummond, *Bioinformatics*, 2012, **28**, 1647-1649.
12. K. Katoh and D. M. Standley, *Mol. Biol. Evol.* , 2013, **30**, 772-780.
13. L.-T. Nguyen, H. A. Schmidt, A. Von Haeseler and B. Q. Minh, *Mol. Biol. Evol.* , 2015, **32**, 268-274.
14. D. T. Hoang, O. Chernomor, A. Von Haeseler, B. Q. Minh and L. S. Vinh, *Mol. Biol. Evol.* , 2018, **35**, 518-522.
15. A. T. Smith, N. Santama, S. Dacey, M. Edwards, R. C. Bray, R. N. Thorneley and J. F. Burke, *J. Biol. Chem.*, 1990, **265**, 13335-13343.
16. Y. Miki, M. Morales, F. J. Ruiz-Dueñas, M. J. Martínez, H. Wariishi and A. T. Martínez, *Protein Expr. Purif.*, 2009, **68**, 208-214.
17. J. Shigeto, Y. Itoh, Y. Tsutsumi and R. Kondo, *FEBS J.*, 2012, **279**, 348-357.
18. G. Zhao, Y.-Y. Guo, S. Yao, X. Shi, L. Lv and Y.-L. Du, *Nat. Commun.*, 2020, **11**, 1614.
19. B. E. Saltzman, *Anal. Chem.*, 1954, **26**, 1949-1955.